

Global Structural Optimization of Tungsten Borides

Quan Li,^{1,2} Dan Zhou,^{1,2} Weitao Zheng,¹ Yanming Ma,^{1,*} and Changfeng Chen^{2,†}

¹College of Materials Science and Engineering, State Key Laboratory of Superhard Materials, Jilin University, Changchun 130012, China

²Department of Physics and High Pressure Science and Engineering Center, University of Nevada, Las Vegas, Nevada 89154, USA

(Received 7 December 2012; published 27 March 2013)

Tungsten borides are among a distinct class of transition-metal light-element compounds with superior mechanical properties that rival those of traditional superhard materials. An in-depth understanding of these compounds, however, has been impeded by uncertainties regarding their complex crystal structures. Here, we examine a wide range of chemical compositions of tungsten borides using a recently developed global structural optimization approach. We establish thermodynamically stable structures and identify a large number of metastable phases. These results clarify and correct previous structural assignments and predict new structures for possible synthesis. Our findings provide crucial insights for understanding the rich and complex crystal structures of tungsten borides, which have broad implications for further exploration of this class of promising materials.

DOI: [10.1103/PhysRevLett.110.136403](https://doi.org/10.1103/PhysRevLett.110.136403)

PACS numbers: 71.20.Be, 61.50.Ah, 81.05.Zx

Transition-metal light-element compounds have been the focus of intense recent research that has led to the discovery of many new materials with novel properties [1–6]. Recent synthesis of boron-rich tungsten borides [7–9] has reignited great interest in these compounds that show outstanding properties, such as ultra hardness, high melting points, and strong resistance to oxidation and acids, that rival or exceed those of traditional superhard materials [10–18]. Past studies have identified five stoichiometric compositions, W_2B (γ -phase) [19,20], WB (α -WB or δ -WB) [19,21], WB_2 (AlB_2 structure) [22], W_2B_5 (ϵ -phase) [19,23], and WB_4 [7–9]. It has, however, been difficult to determine the crystal structures of these W_xB_y compounds from experimental x-ray diffraction (XRD) patterns due to the small scattering cross section of boron atoms, and this situation is compounded by the existence of numerous structural configurations stemming from the versatile ability of boron atoms to form sp , sp^2 , and sp^3 hybridized and even multicenter bonds [24–26]. Previous attempts have mostly used empirical approaches in selecting and modifying known crystal structures to fit the experimental XRD data, but such *ad hoc* approaches have produced a hit-and-miss record that leads to incomplete and often conflicting structural assignments. These structural uncertainties have impeded in-depth understanding and further exploration of these promising materials. It is a pressing task to resolve the complex structures of tungsten borides across a wide range of chemical composition, which would help clarify experimental results and predict new crystal phases for synthesis.

In this work, we employ a systematic first-principles global structural optimization method to search and identify the structures of tungsten borides. We obtain a comprehensive set of structures for each composition, and

the results confirm several W_xB_y structures that were previously proposed and correct others that were erroneously assigned. In particular, we establish for the first time the thermodynamically stable structures for W_2B , W_2B_5 , and WB_3 . Equally important, our work identifies a large number of low-lying metastable structures that stem from the versatile bonding ability of boron atoms. These metastable structures are energetically competitive and may be synthesized under proper conditions. The present results provide insights and a road map for exploring design and synthesis strategies for new W_xB_y compounds. Such knowledge is also key to understanding other transition-metal light-element compounds that face similar challenges concerning structural determination.

Our global structural optimization used the CALYPSO code with a variable-cell particle-swarm optimization algorithm [27,28], which has successfully predicted structures of various systems ranging from elemental solids to binary and ternary compounds [29–34]. The energetic calculations were carried out using the density functional theory with the Perdew-Burke-Ernzerh generalized gradient approximation [35] exchange-correlation potential as implemented in the VASP code [36]. The electron-ion interaction was described by means of projector augmented wave [37] with $5d^46s^2$ and $2s^22p^1$ electrons as valence for W and B atoms, respectively. The electronic wave functions were expanded in a plane-wave basis set with a cutoff energy of 450 eV for all cases. Monkhorst-Pack k point meshes with a grid of 0.025 \AA^{-1} for Brillouin zone sampling were chosen to achieve the total energy convergence of less than 1 meV/atom. To determine the dynamical stability of the studied structures, we performed phonon calculations by the direct supercell method using the forces obtained by the Hellmann-Feynman theorem [38,39].

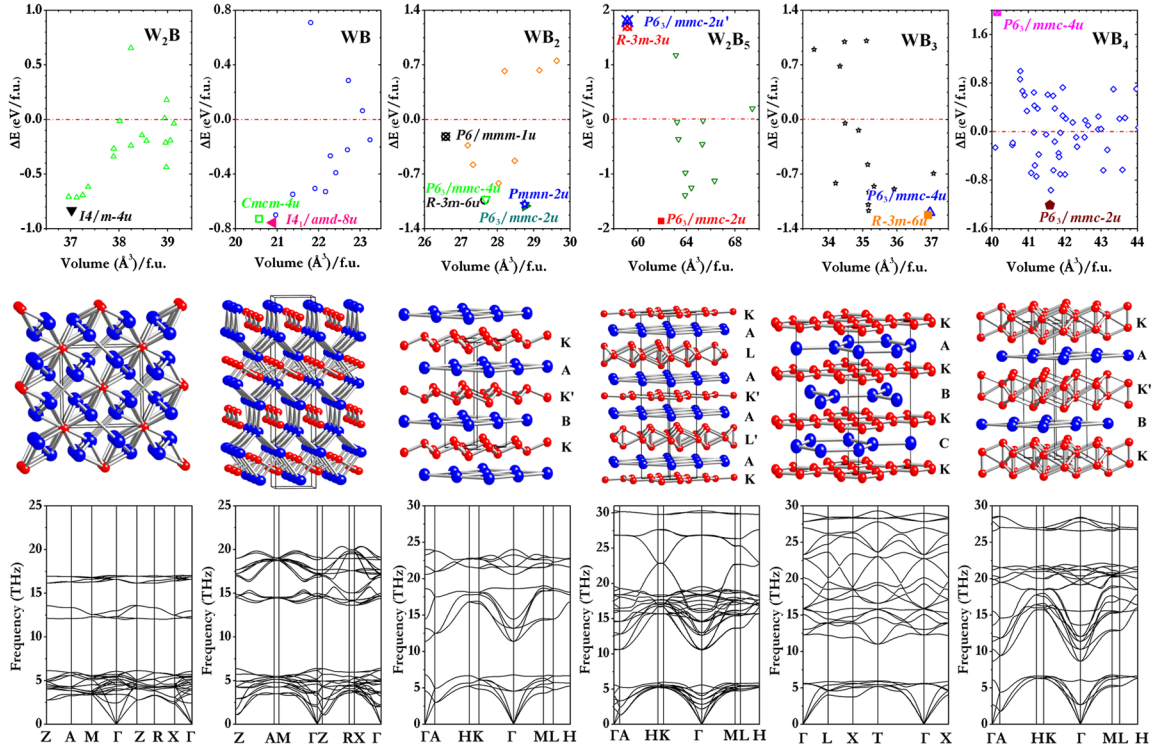


FIG. 1 (color online). Top row: Calculated formation enthalpy and equilibrium volume of tungsten borides predicted by our global structural search for W_2B , WB , WB_2 , W_2B_5 , WB_3 , and WB_4 . Each symbol represents an individual structure, and some key structures are highlighted to facilitate discussion (see main text for details). Middle row: Thermodynamically stable structures for each stoichiometry (left to right): $I4/m-4u$ W_2B , $I4_1/amd-8u$ WB , $P6_3/mmc-2u$ WB_2 , $P6_3/mmc-2u$ W_2B_5 , $R-3m-6u$ WB_3 , and $P6_3/mmc-2u$ WB_4 [47]. The large (blue) and small (red) spheres represent W and B atoms, respectively. Bottom row: Calculated phonon band structures of the six thermodynamically stable structures shown above (same order).

Our structural search yields a large number of tungsten boride structures as shown in Fig. 1. The stability of the predicted W_xB_y structures is quantified using the formation enthalpy defined by $\Delta E = E_{W_xB_y} - xE_W - yE_B$, where a negative ΔE indicates stability or metastability of a structure. These rich and complex crystal structures stem from the strong ability of boron atoms to form a variety of bonds that produce versatile structural patterns [24,25]. In particular, structures on the boron-rich side contain alternating sandwichlike boron and metal layers with different stacking sequences. The honeycomb boron sheets in boron-rich compounds are chemically rationalized by the elevated B anionic charge resulting from the $W \rightarrow B$ charge transfer. The thermodynamically stable structures for each composition are presented together with their phonon dispersion curves that all show no sign of imaginary phonon modes in the entire Brillouin zone, thus confirming their dynamic stability. In Fig. 2, we plot the enthalpy of the most stable structure of tungsten borides at each composition (the convex hull); also shown are several previously proposed structures that are identified by our calculations to be metastable or unstable (see discussions below). A structure whose formation enthalpy lies on the convex hull, which can be considered as the global stability line, is deemed stable with respect to decomposition into other borides or

elemental solids and thus may be experimentally synthesized in principle [40,41]. The formation enthalpy data of $I4/m-4u$ W_2B , $I4_1/amd-8u$ WB , $P6_3/mmc-2u$ WB_2 , $R-3m-6u$ WB_3 , and $P6_3/mmc-2u$ WB_4 sit right on the convex hull, while that of $P6_3/mmc-2u$ W_2B_5 is slightly above the convex hull. Here nu denotes that the structure contains n formula units (f.u.) per unit cell ($n = 1-8$). Below, we clarify and correct previously proposed structures and predict new crystal phases of tungsten borides.

The synthesized W_2B (γ - W_2B) has long been thought to have tetragonal Al_2Cu -type structure with space group $I4/mcm$ (denoted as $I4/mcm-4u$) [20,42,43]. Our search, however, identified a different tetragonal structure with space group $I4/m$ ($I4/m-4u$) as the thermodynamically stable phase for W_2B , which is 2 meV/f.u. lower in enthalpy than $I4/mcm-4u$. The equilibrium lattice parameters of the $I4/m-4u$ structure are $a = b = 5.580 \text{ \AA}$, $c = 4.756 \text{ \AA}$ with W at Wyckoff $8h$ (0.17646, 0.66390, 0.0) and B at $4e$ (0.0, 0.0, 0.22105) positions. Each boron atom forms an eightfold coordinate with tungsten atoms with two similar bond distances of 2.365 and 2.420 \AA , while each tungsten atom is surrounded by four boron atoms and three tungsten atoms. The metallic W-W bonds also have two nearly equal bond distances of 2.688 and 2.693 \AA , which are slightly smaller than that in pure

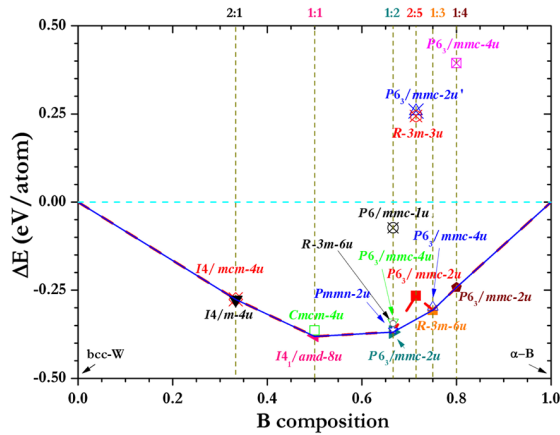


FIG. 2 (color online). The formation enthalpy versus composition for stoichiometric tungsten borides with bcc-W and α -B as the reference states. The solid line denotes the ground-state convex hull.

tungsten metal (2.747 Å). In addition to the energetic considerations, our phonon calculations show that the frequency of a transverse acoustic (TA) mode is imaginary at the BZ center (Γ point) in the $I4/mcm-4u$ structure [Fig. 3(a)], whereas no imaginary phonon frequencies appear in the $I4/m-4u$ structure [Fig. 3(b)]. This shows that $I4/mcm-4u$ W_2B is dynamically unstable. We further performed frozen-phonon calculations [44] to track the atomic movement associated with the soft phonon modes of $I4/mcm-4u$ W_2B . A schematic illustration of the eigenvectors for the soft TA mode at the Γ point of the $I4/mcm-4u$ structure is shown in Fig. 3(c), where the arrows indicate the directions of the atomic vibrations.

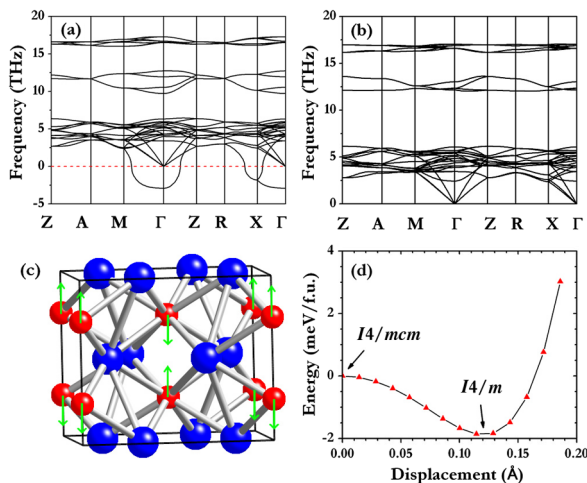


FIG. 3 (color online). Phonon dispersion curves for (a) $I4/mcm-4u$ W_2B and (b) $I4/m-4u$ W_2B . The movements of boron atoms (smaller red spheres) along the eigenvector of the soft TA (Γ) mode in the $I4/mcm-4u$ cell of W_2B are indicated by the arrows in (c), and the corresponding energy evolution, relative to that of $I4/mcm-4u$ W_2B , with the boron atom displacements is shown in (d).

The total energy for a series of atomic displacement along the vibration direction of the soft TA (Γ) mode was then calculated and plotted in Fig. 3(d). The stabilization of a new phase is evidenced by the energy minimum at an atomic distortion of 0.12 Å. A structural optimization of this new phase with respect to atomic distortions at the energy minimum yields the tetragonal $I4/m-4u$ phase predicted by our structural search.

Monoboride WB has been reported to exist in two forms: the low-temperature tetragonal α -WB ($I4_1/amd-8u$, or δ -WB) structure and the high-temperature orthorhombic β -WB ($Cmcm$, $Cmcm-4u$) [20,42,43]. Our calculations show that the most stable WB phase is $I4_1/amd-8u$, thus confirming previously proposed assignment. A close examination of structural details show that alternate zigzag chains of boron atoms run in the [100] and [010] crystallographic directions in $I4_1/amd-8u$ WB, while all zigzag chains of boron atoms align in the [100] direction in the $Cmcm-4u$ structure. Each boron chain is surrounded by hexagonal tungsten atoms in both $I4_1/amd-8u$ and $Cmcm-4u$ WB. Because of the similar bonding features in these two structures, the energy of $I4_1/amd-8u$ WB is ~ 0.015 eV/atom lower than that of the orthorhombic β -WB ($Cmcm-4u$). This explains the experimental observation that β -WB can be synthesized only at high temperatures.

The crystal structure for WB_2 was long believed to be hexagonal $A1B_2$ -type ($P6/mmm-1u$) [22]. Our calculations show, however, that its enthalpy is 0.286 eV per atom above the ground-state structure (see Fig. 1). Furthermore, phonon calculations reveal that $P6/mmm-1u$ WB_2 has imaginary frequencies and thus is dynamically unstable. Our structural search identifies a hexagonal ReB_2 - WB_2 ($P6_3/mmc-2u$) phase as the most stable structure, which agrees with the conclusion of recent studies [10,15]. This phase lies on the calculated convex hull and possesses the lowest formation enthalpy per atom on the boron-rich side of the phase diagram (see Fig. 2). Its sacking puckered boron sheets and close-packed sequence of W layers is arranged in $KAK'B\dots$ along the c axis. A recent study [10] proposed several other candidate WB_2 structures, including hexagonal $P6_3/mmc-4u$, rhombohedral $R-3m-6u$, and orthorhombic RuB_2 -type $Pmnm-2u$. Our energetic and phonon calculations confirm that these are all metastable phases with dynamical stability and thus may be synthesized under proper conditions (e.g., at high temperature).

The ϵ phase was initially thought to be in hexagonal ($P6_3/mmc-2u'$) or rhombohedral ($R-3m-3u$) W_2B_5 structure [19]. However, recent studies identified it as stoichiometric tungsten diboride W_2B_4 crystallized in WB_2 -type structure [13]. Meanwhile, our structural search predicts that the most stable W_2B_5 phase is hexagonal $P6_3/mmc-2u$ with stacking sequence of $KALAK'AL'A\dots$ along the c axis. The boron atoms between the simple hexagonal W layers form two different types of structures: the $K(K')$ type that is a slightly buckled honeycomb sheet and the $L(L')$

type that is a wrinkled graphitelike layer with half of the boron atoms each replaced by a pair of vertical B_2 dimers. Our calculations show that the previously proposed $P6_3/mmc-2u'$ and $R-3m-3u$ structures have positive formation enthalpies of 0.258 and 0.244 eV/atom, respectively and, thus, are not energetically viable.

Recently synthesized tungsten tetraboride (WB_4) has the highest reported boron content with a microhardness of 43–46 GPa under the load of 0.49 N, which makes it the most promising candidate as a superhard material among transition-metal borides [7–9]. The structural identification of WB_4 has generated considerable interest and controversy. WB_4 was initially assumed to be in a hexagonal WB_4 -type structure ($P6_3/mmc-4u$) [45]. Recent studies, based on analysis of thermodynamic and lattice stabilities, suggested that the synthesized material should be characterized as WB_3 ($P6_3/mmc-4u$) [11,12], which can be regarded as defective WB_4 with one of the four boron atoms at $4f$ sites removed from WB_4 , thus possessing the same symmetry. However, a recent study of mechanical properties of WB_3 raised additional questions regarding its structural assignment [46]. Our structural search predicts $R-3m-6u$ WB_3 and $P6_3/mmc-2u$ WB_4 as the ground-state structures that are energetically more favorable by 0.008 and 0.663 eV/atom than the previously proposed $P6_3/mmc-4u$ WB_3 and $P6_3/mmc-4u$ WB_4 , respectively. Both $R-3m-6u$ and $P6_3/mmc-4u$ WB_3 can be considered as the superlattice of $P6/mmm-1u$ WB_2 with one third of W atoms removed. The stacking sequence of the planar graphitelike boron sheet in $R-3m-6u$ WB_3 is identical to that in $P6_3/mmc-4u$ WB_3 . Their difference lies in the stacking sequence of the honeycomb tungsten layers that is $ABC\dots$ in $R-3m-6u$ WB_3 but $ABAB\dots$ in $P6_3/mmc-4u$ WB_3 .

We have simulated the XRD data of the ground-state and energetically competitive metastable structures of tungsten borides with various chemical compositions and compared them to available experimental data. This screening process selects the structures that best describe the synthesized materials. The XRD data of the γ phase is best fit by our newly identified $I4/m-4u$ W_2B structure [Fig. 4(a)]; the presence of a few extra minor peaks is attributed to the coexisting α -phase WB in the synthesized sample [20]. The best fit to the XRD data of the α phase comes from the $I4_1/amd-8u$ WB [Fig. 4(b)]. In both cases, the synthesized compounds adopt the thermodynamically stable structures. For the ϵ phase, however, its XRD pattern is best fit by the $P6_3/mmc-4u$ WB_2 structure that is a metastable structure [Fig. 4(c)]. A similar situation occurs for the recently synthesized nominal WB_4 [7,8]. Among all the structures obtained by our search process, only the metastable $P6_3/mmc-4u$ WB_3 matches the experimental XRD data [Fig. 4(d)]. These metastable phases differ from their thermodynamically stable counterparts (see Fig. 1) either in stacking sequence or in subtle changes in boron layer sliding and buckling, which stem from the versatile bonding ability of boron atoms. At the fundamental level, it indicates that

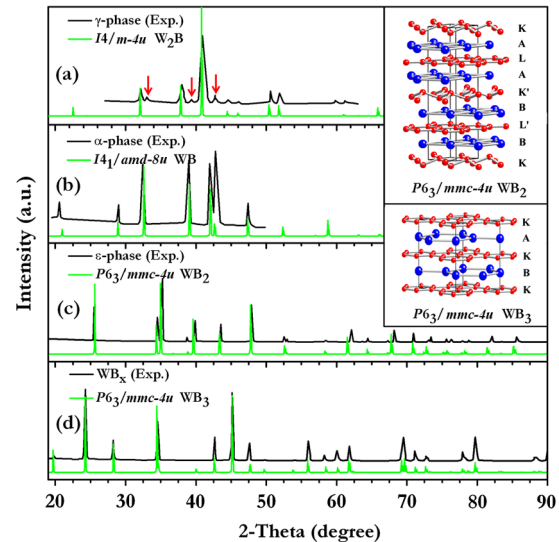


FIG. 4 (color online). Matching simulated XRD patterns of $I4/m-4u$ W_2B , $I4_1/amd-8u$ WB, $P6_3/mmc-4u$ WB_2 , and $P6_3/mmc-4u$ WB_3 (x-ray wavelength $\lambda = 1.54056$ Å) with experimental data for (a) γ phase [20], (b) α phase [21], (c) ϵ phase [23], and (d) WB_x [7], respectively. Arrows in (a) mark the appearance of the α phase coexisting with the γ phase. The crystal structures of the metastable phases $P6_3/mmc-4u$ WB_2 and $P6_3/mmc-4u$ WB_3 are shown in the insets [47].

the energy landscape has become more complicated as boron concentration rises, and the local minima in the energy landscape are capable of trapping and maintaining metastable structures under the experimental synthesis conditions. This suggests that, under proper sample preparation and synthesizing conditions, other metastable tungsten borides may also be obtained given the large number of new structures with negative formation enthalpy identified by the present work. More importantly, the calculated convex hull (Fig. 2) shows that the thermodynamically stable $P6_3/mmc-2u$ WB_2 , $R-3m-6u$ WB_3 , and $P6_3/mmc-2u$ WB_4 that have not yet been synthesized are stable with respect to decomposition into other borides or elemental solids and thus should be accessible to synthesis. These findings may lead to new discoveries of more tungsten boride phases, especially on the boron-rich side of the phase diagram, producing a significantly expanded family of tungsten borides with more diverse and useful properties.

In summary, we have performed a systematic global structural optimization of tungsten borides and identified the thermodynamically stable structures as well as a large number of metastable structures over a wide range of boron concentrations. These results provide a blueprint for analyzing a variety of tungsten borides and offer a useful guide for characterizing existing W-B compounds and potentially synthesizing many new ones. Comparison of experimental and simulated x-ray diffraction patterns leads to the identification of previously synthesized $I4/m-4u$ W_2B , $I4_1/amd-8u$ WB, $P6_3/mmc-4u$ WB_2 , and $P6_3/mmc-4u$

WB₃. On the basis of the calculated convex hull, we predict that $P6_3/mmc-2u$ WB₂, $R-3m-6u$ WB₃, and $P6_3/mmc-2u$ WB₄ are thermodynamically stable and thus viable for experimental synthesis. Additional metastable phases with various compositions may also be synthesized. Our results are expected to stimulate new material exploration and discovery, and the method used in the present Letter is also applicable to exploring the rich and complex structures of other transition-metal light-element compounds.

The work was supported by the DOE under Grant No. DE-FC52-06NA26274 at UNLV and by NNSF of China under Grants No. 11025418, No. 91022029, and No. 51202084 at JLU.

*mym@jlu.edu.cn

†chen@physics.unlv.edu

- [1] J. C. Crowhurst, A. F. Goncharov, B. Sadigh, C. L. Evans, P. G. Morrall, J. L. Ferreira, and A. J. Nelson, *Science* **311**, 1275 (2006).
- [2] E. Gregoryanz, C. Sanloup, M. Somayazulu, J. Badro, G. Fiquet, H.-k. Mao, and R. J. Hemley, *Nat. Mater.* **3**, 294 (2004).
- [3] A. F. Young, C. Sanloup, E. Gregoryanz, S. Scandolo, R. Hemley, and H.-k. Mao, *Phys. Rev. Lett.* **96**, 155501 (2006).
- [4] S. H. Tolbert, M. B. Weinberger, J. J. Gilman, S. M. Clark, S. H. Tolbert, and R. B. Kaner, *J. Am. Chem. Soc.* **127**, 7264 (2005).
- [5] H. Y. Chung, M. B. Weinberger, J. B. Levine, A. Kavner, J.-M. Yang, S. H. Tolbert, and R. B. Kaner, *Science* **316**, 436 (2007).
- [6] J. Q. Qin, D. He, J. Wang, L. Fang, L. Lei, Y. Li, J. Hu, Z. Kou, and Y. Bi, *Adv. Mater.* **20**, 4780 (2008).
- [7] R. Mohammadi, A. T. Lech, M. Xie, B. E. Weaver, M. T. Yeung, S. H. Tolbert, and R. B. Kaner, *Proc. Natl. Acad. Sci. U.S.A.* **108**, 10958 (2011).
- [8] M. Xie, R. Mohammadi, Z. Mao, M. M. Armentrout, A. Kavner, R. B. Kaner, and S. H. Tolbert, *Phys. Rev. B* **85**, 064118 (2012).
- [9] Q. Gu, F. Krauss, and W. Steurer, *Adv. Mater.* **20**, 3620 (2008).
- [10] E. Zhao, J. Meng, Y. Ma, and Z. Wu, *Phys. Chem. Chem. Phys.* **12**, 13 158 (2010).
- [11] R. F. Zhang, D. Legut, Z. J. Lin, Y. S. Zhao, H. K. Mao, and S. Veprek, *Phys. Rev. Lett.* **108**, 255502 (2012).
- [12] H. Gou, Z. Li, L. M. Wang, J. Lian, and Y. Wang, *AIP Adv.* **2**, 012171 (2012).
- [13] M. Frotscher, W. Klein, J. Bauer, C.-M. Fang, J.-F. Halet, A. Senyshyn, C. Baehtz, and B. Albert, *Z. Anorg. Allg. Chem.* **633**, 2626 (2007).
- [14] Y. Liang, X. Yuan, and W. Zhang, *Phys. Rev. B* **83**, 220102 (2011).
- [15] X.-Q. Chen, C. L. Fu, M. Krčmar, and G. S. Painter, *Phys. Rev. Lett.* **100**, 196403 (2008).
- [16] S. A. Gromilov, S. A. Kinelovskii, A. V. Alekseev, and I. B. Kirienko, *J. Struct. Chem.* **51**, 1126 (2010).
- [17] J. Yang, H. Sun, and C. Chen, *J. Am. Chem. Soc.* **130**, 7200 (2008).
- [18] C. Zang, H. Sun, J. S. Tse, and C. Chen, *Phys. Rev. B* **86**, 014108 (2012).
- [19] R. Kiessling, *Acta Chem. Scand.* **1**, 893 (1947).
- [20] H. Itoh, T. Matsudaira, S. Naka, H. Hamamoto, and M. Obayashi, *J. Mater. Sci.* **22**, 2811 (1987).
- [21] S. Okada, K. Kudou, and T. Lundström, *Jpn. J. Appl. Phys.* **34**, 226 (1995).
- [22] H. P. Woods, F. E. Wagner, Jr., and B. G. Fox, *Science* **151**, 75 (1966).
- [23] M. Kayhan, E. Hildebrandt, M. Frotscher, A. Senyshyn, K. Hofmann, L. Alff, and B. Albert, *Solid State Sci.* **14**, 1656 (2012).
- [24] A. R. Oganov and V. L. Solozhenko, *J. Superhard Mater.* **31**, 285 (2009).
- [25] A. R. Oganov, J. Chen, C. Gatti, Y. Ma, Y. Ma, C. W. Glass, Z. Liu, T. Yu, O. O. Kurakevych, and V. L. Solozhenko, *Nature (London)* **457**, 863 (2009).
- [26] W. Zhou, H. Sun, and C. Chen, *Phys. Rev. Lett.* **105**, 215503 (2010).
- [27] Y. Wang, J. Lv, L. Zhu, and Y. Ma, *Phys. Rev. B* **82**, 094116 (2010).
- [28] Y. Wang, J. Lv, L. Zhu, and Y. Ma, *Comput. Phys. Commun.* **183**, 2063 (2012).
- [29] J. Lv, Y. Wang, L. Zhu, and Y. Ma, *Phys. Rev. Lett.* **106**, 015503 (2011).
- [30] L. Zhu, Z. Wang, Y. Wang, G. Zou, H. Mao, and Y. Ma, *Proc. Natl. Acad. Sci. U.S.A.* **109**, 751 (2012).
- [31] H. Wang, J. Tse, K. Tanaka, T. Iitaka, and Y. Ma, *Proc. Natl. Acad. Sci. U.S.A.* **109**, 6463 (2012).
- [32] Y. Wang, H. Liu, J. Lv, L. Zhu, H. Wang, and Y. Ma, *Nat. Commun.* **2**, 563 (2011).
- [33] L. Zhu, H. Wang, Y. Wang, J. Lv, Y. Ma, Q. Cui, Y. Ma, and G. Zou, *Phys. Rev. Lett.* **106**, 145501 (2011).
- [34] Q. Li, H. Liu, D. Zhou, W. T. Zheng, Z. Wu, and Y. Ma, *Phys. Chem. Chem. Phys.* **14**, 13 081 (2012).
- [35] J. P. Perdew, K. Burke, and M. Ernzerhof, *Phys. Rev. Lett.* **77**, 3865 (1996).
- [36] G. Kresse and J. Furthmüller, *Phys. Rev. B* **54**, 11 169 (1996).
- [37] G. Kresse and D. Joubert, *Phys. Rev. B* **59**, 1758 (1999).
- [38] A. Togo, F. Oba, and I. Tanaka, *Phys. Rev. B* **78**, 134106 (2008).
- [39] A. Togo, F. Oba, and I. Tanaka, *Phys. Rev. B* **77**, 184101 (2008).
- [40] X. Zhang, G. Trimarchi, and A. Zunger, *Phys. Rev. B* **79**, 092102 (2009).
- [41] G. Ghosh, A. Van de Walle, and M. Asta, *Acta Mater.* **56**, 3202 (2008).
- [42] B. Armas and F. Trombe, *Sol. Energy Mater.* **15**, 67 (1973).
- [43] S. Stadler, R. P. Winarski, J. M. MacLaren, D. L. Ederer, J. vanEk, A. Moewes, M. M. Grush, T. A. Callcott, and R. C. C. Perera, *J. Electron Spectrosc. Relat. Phenom.* **110**, 75 (2000).
- [44] L. Zhang, Y. Wang, T. Cui, Y. Li, Y. Li, Z. He, Y. Ma, and G. Zou, *Phys. Rev. B* **75**, 144109 (2007).
- [45] P. A. Romans and M. P. Krug, *Acta Crystallogr.* **20**, 313 (1966).
- [46] C. Zang, H. Sun, and C. Chen, *Phys. Rev. B* **86**, 180101 (2012).
- [47] See Supplemental Material at <http://link.aps.org/supplemental/10.1103/PhysRevLett.110.136403> for structural details of these tungsten borides.